Power Optimization of Wind Electric Conversion Systems Integrated into the Utility Grid.

Konstantine Kalaitzakis and George Vachtsevanos.
School of Engineering, Democritus University of Thrace, Xanthi, Greece.

Abstract

This paper is concerned with the interconnected operation of WECS with the utility grid. Specifically, it addresses problems of stability, protection and power flow optimization from the WECS to the power lines.

The approach followed contains both a theoretical and an experimental component. A variable-speed constant-frequency wind electric system utilizing a synchronous generator and line-commutated inverter provides experimental verification of computer simulation studies for the dynamic and steady-state performance of the interconnected system.

Simulation results indicate that the transient behavior of the wind electric-power grid system is satisfactory with appropriate devices providing adequate protection to both the wind generator and the utility grid from a variety of fault conditions.

A maximum power tracking mechanism has been designed for the continuous matching of the wind-electric generator to the grid impedance characteristics. As a result, maximum electric power is transferred from the wind machine to the power lines. Computer simulation studies of this type of operation indicate the substantial improvement in power transfer that is achieved.

The proposed scheme tends to minimize equipment and maintenance costs while maximizing the energy transfer capabilities of the wind-electric conversion system and maintaining a high degree of reliability in overall system performance.

1. Introduction

In recent years there has been growing interest in utilizing wind-electric conversion systems to provide some of the electricity demand on a large scale [1]. Such systems are usually interfaced with the existing power grid for "fuel displacement" purposes as well as for earning some "capacity credit". In the case of an autonomous operation of WECS, some form of energy storage is required (pumped storage, hydrogen production or battery storage) thus reducing the economic attractiveness of the overall system.

This work involves the study of grid interface problems associated with the parallel operation of WECS and conventional power stations interconnected with the utility grid [2-8]. The technoeconomic requirements for the reliable operation of WECS interconnected with the power grid may be summarized in the following statements [9]:

1. The wind generator system must have a high degree of efficiency for the whole region of power output operation.
2. The grid must be capable of absorbing, at each instant of time, the maximum power produced by the wind generator system.
3. The electrical power must be introduced into the grid without distortion and should not require a reactive power component.
4. The unscheduled interruption of the operation of one wind generator or more should not disturb the operating characteristics of the utility system.
5. Faults on the WECS side should not interfere with the overall stability of the power system.
6. The operation of the WECS should be reliable and should involve the minimum possible maintenance requirements.

In the operation of a wind-powered generator, power in the wind (P_W) is converted to mechanical power (P_M) by the aerodynamic system and is then converted to its electrical form (P_e) by the electrical generating system, as shown in Figure 1.

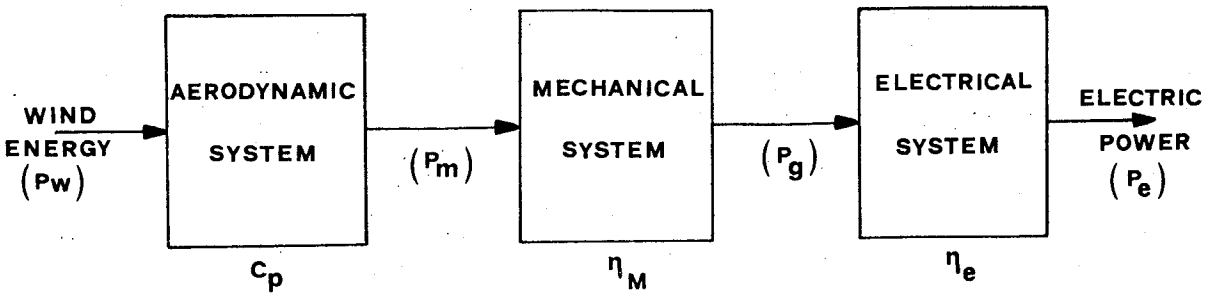

Figure 1 Block diagram of the WECS components

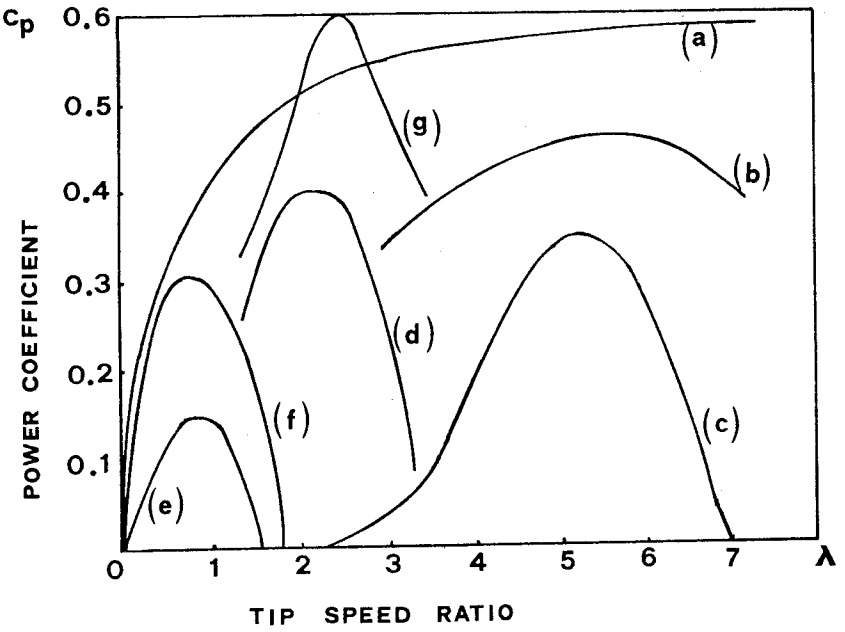

Figure 2 Power coefficient C_p vs. wind speed ratio λ for various types of turbines

(a) Ideal efficiency of propeller type turbine
(b) High speed two or three blade turbine
(c) Darrieus rotor
(d) Modern multiblade turbine
(e) American farm windmill
(f) Savonius rotor
(g) Cyclogiro wind turbine

The mechanical power developed, P_M, is given by $P_M = C_p P_W$, where C_p is the power coefficient representing efficiency of conversion from wind power to mechanical power. The dependence of this coefficient on the ratio of rotor blade tip speed to wind speed, λ, is shown in Figure 2. The characteristic curves for various types of wind generators indicate that if the turbine's rated speed corresponds to the maximum value of C_p, then increasing or decreasing wind speed will result in decreasing C_p if the shaft speed is held constant. On the other hand, if rotor speed is allowed to vary with wind speed, maximum C_p could be realized for a wide range of operating wind speeds. Thus, two basic schemes have evolved for wind-electric conversion systems: those that operate under constant-speed constant-frequency (CSCF) conditions and those that operate at variable shaft speed but constant electrical frequency (VSCF).

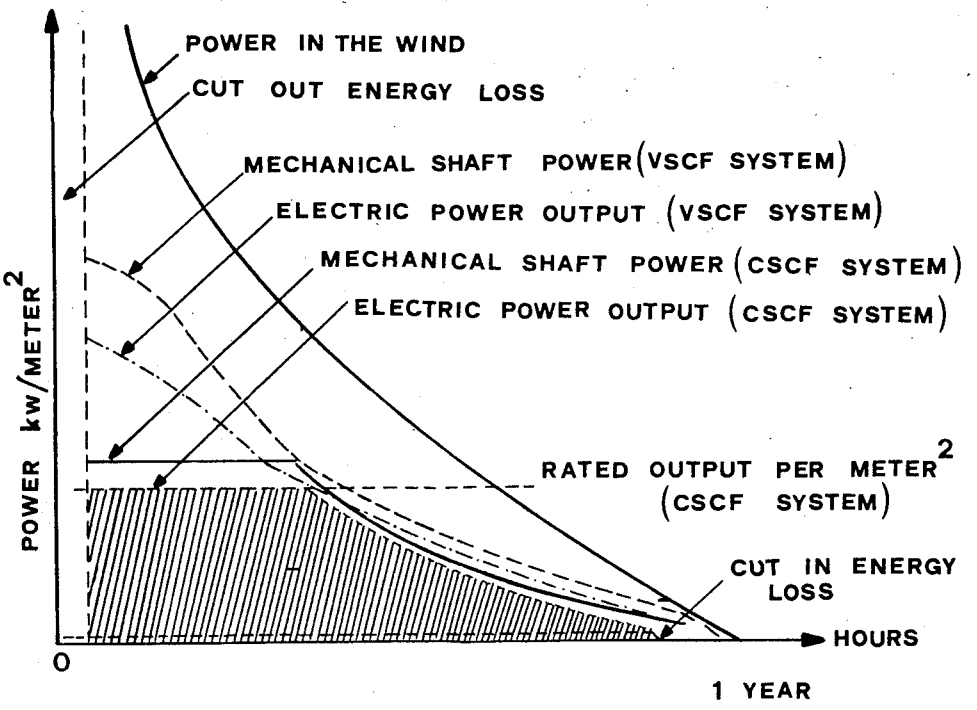

Figure 3 Power duration curves for CSCF and VSCF schemes

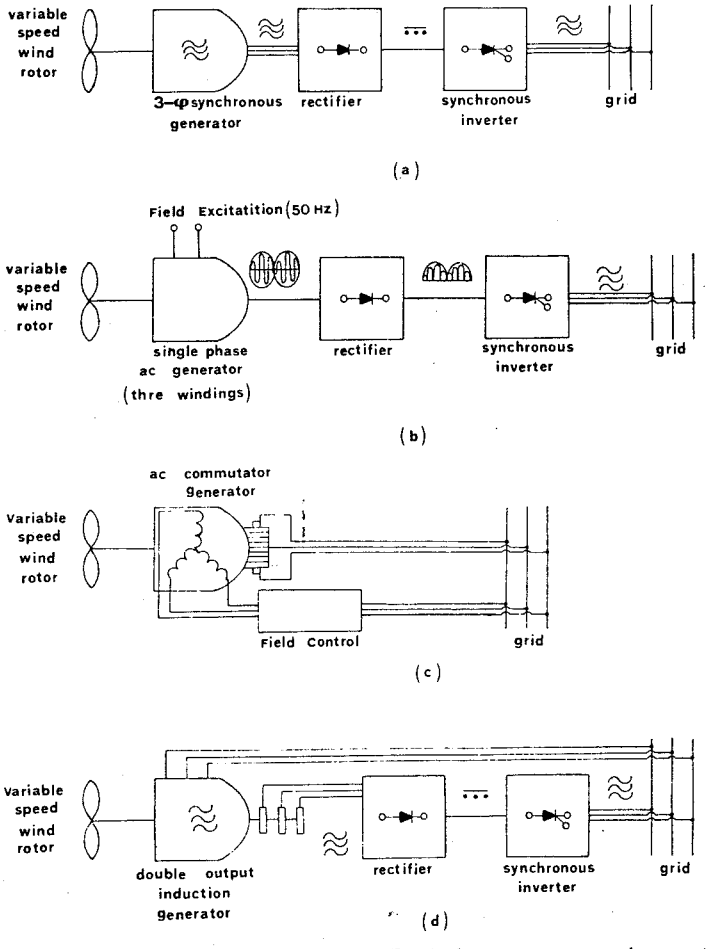

Figure 4 Alternative techniques for VSCF wind energy conversion systems connected to the grid

Figure 3 shows that the electric energy generated per year by prevailing winds is generally higher for VSCF wind-electric systems than for CSCF systems, since the former may allow operation at power outputs above the rated value at high wind speeds.

CSCF systems usually employ synchronous wind-powered generators operating in parallel with the power grid (similar to the system used in hydropower stations), or induction machines operating with small slip above synchronous speed. Because of the intermittent nature of wind energy, synchronous generators require complex and expensive control mechanisms to vary the pitch of the rotor so that the power derived from the wind energy is held fairly constant. Induction generators, on the other hand, require additional power factor improvement equipment and some means of providing field excitation. Stability problems can also arise in both types, requiring the installation of appropriate protective devices.

Variable-speed constant-frequency systems are characterized by a rotor allowed to rotate freely with the wind. Various VSCF schemes have been proposed and four typical situations are shown in Figure 4. In methods (a) and (b) the generator shaft, rotating at varying speeds following the speed of the wind, is coupled to an ac generator with dc or ac excitation. The result is a variable frequency output as compared to the constant frequency of the power grid, and this must be processed electronically so that it may be "synchronized" to the frequency characteristics of the utility system. The third method (c) utilizes an ac commutator generator with field excitation derived from the grid. Because of the commutator, the machine's output frequency is equal to the excitation frequency and therefore it may be connected back directly to the grid. The last method (d) uses a double-output induction generator operating at varying speeds and supplying line-frequency power directly to the grid through stator windings and indirectly through the rotor after processing electronically the slip-frequency power.

An advantage of the VSCF systems relates to the possibility of controlling such operating characteristics as generator output impedance and shaft speed in a manner that maximizes their efficiency. Control of the generator speed may achieve a value of the ratio λ which maximises the power coefficient C_p for a turbine at any wind speed. Control of the output impedance of the generator, on the other hand, may achieve a matching with the grid impedance at the point of connection. The economic benefits from such an optimized operation of WECS interconnected with the power grid are obvious if one considers the strong dependence of the mechanical power output on wind speed keeping in mind the typical wind speed frequency distribution characteristics.

On the basis of the "optimized design" philosophy, several schemes have been proposed to take advantage of the features mentioned in the previous paragraph. Field modulated generator systems with a control scheme employing wind speed and shaft speed, or torque and shaft speed, as the control inputs have been designed [11] so that the ratio λ is kept constant at a value which maximizes the power coefficient C_p, thus maintaining a high generator efficiency over a wide range of outputs. Another possible design involves a double-output induction generator as shown in Figure 4(d), with a microprocessor-based controller for the slip-frequency rotor power [1].

The approach reported in this paper is based upon the design of an appropriate controller which tracks the generator output power and modifies the grid interface equipment of a VSCF system in such a way that maximum electrical power is transferred from the WECS to the grid.

2. System Description

Figure 5 shows a block diagram of the proposed maximum power tracking scheme. The VSCF wind-electric conversion system is of the type shown as case (a) in Figure 4. The WECS is configured on the combination of a conventional low-cost synchronous generator with a line commutated synchronous inverter of novel design and simple construction [13]. The system power output is used as the control signal regulating the operating characteristics of the inverter. This particular configuration has a distinct advantage: it aims at maximizing not only the mechanical power output from the aeroturbine but also the total power from the cascaded subsystems (turbine-generator-rectifier-bridge-inverter-power grid). Consequently, the improvement in power transfer achieved is of significant practical importance.

The design approach used has both a theoretical and an experimental component. The theoretical study consists mainly of computer simulations of the dynamic and steady-state behavior of the interconnected system, while the experimental method involves testing of a particular wind-electric conversion system interfaced to the power grid. Experimental results are compared, on a step by step basis, with those obtained from the simulation studies. This dual nature of the approach allows for an optimum design of system components and verification of theoretical results.

Figure 6 shows a detailed block diagram of the internal organization of the

subsystems comprising the wind-electric conversion components and the grid interface hardware.

In the following paragraphs mathematical descriptions for each one of the basic subsystems are developed to be used in the simulation studies. Numerical values for some of the input parameters of the mathematical models are derived from the experimental configuration.

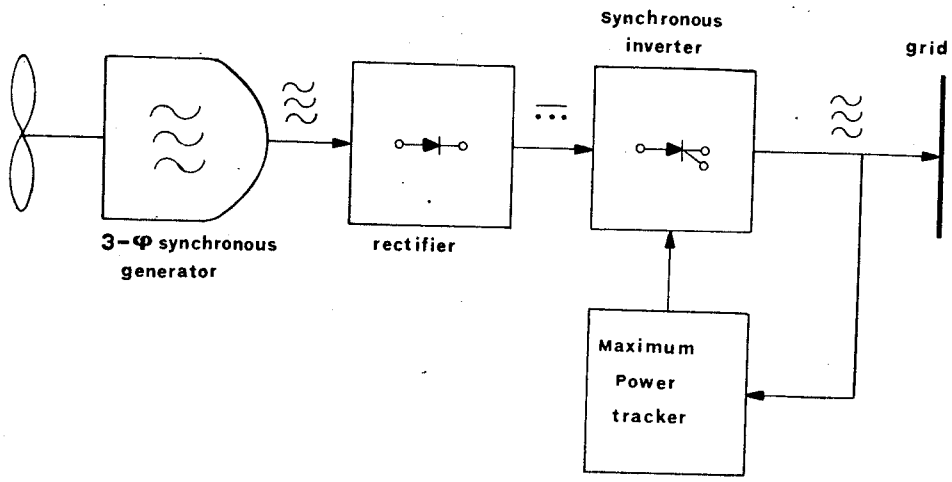

Figure 5 Block diagram of WECS connected to the grid with maximum power tracker

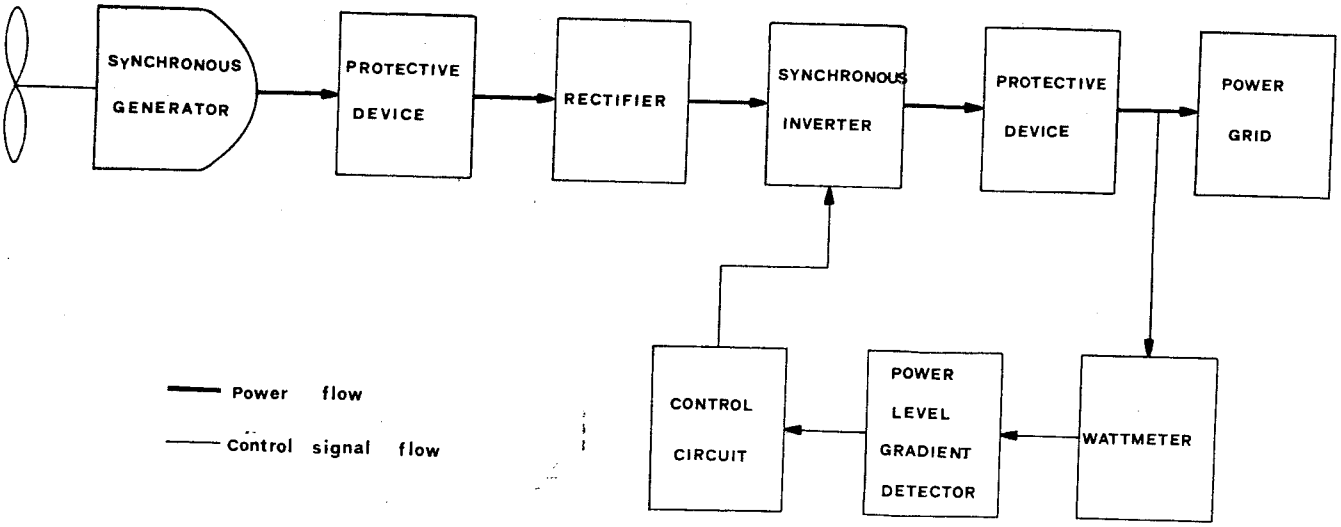

Figure 6 Detailed operational diagram of the interconnected system

(a) The aerodynamic subsystem A two-bladed horizontal axis turbine is used with a propeller diameter of 3 m. The cut-in speed is approximately 3 m/sec and the cut-out speed is about 20 m/sec. The tip speed ratio λ is defined by the relation

$$\lambda = \frac{\omega_p R_p}{V} \tag{1}$$

where ω_p is the propeller angular velocity, R_p the radius of the propeller and V the wind speed. The shaft torque of the propeller is given by

$$T_{IN} = \frac{1}{2} k\rho\pi R_p^3 V^2 C_T \tag{2}$$

where k is a constant, ρ the density of atmospheric air and C_T the torque coefficient. The C_T vs. λ characteristic curve of the experimental wind turbine is approximated by the relation

$$C_T = -0.23\cdot 10^{-5}\lambda^4 + 0.19\cdot 10^{-3}\lambda^3 - 0.01\lambda^2 + 0.16\lambda + 0.25 \tag{3}$$

Equations (1), (2) and (3) define the mathematical model of the wind turbine subsystem. Wind speed V is the input variable and shaft torque T_{IN} the model's output variable with ω_p and intermediate input variable.

(b) The synchronous generator The synchronous generator is a two-pole ac machine with dc excitation. The power output at a rotational speed of 100 rad/sec is 2.5 Kw with a phase voltage of 100 V. Its mathematical description follows Park's classical model for a synchronous machine with a Blondel transformation to a two-phase generator.

The electrical behavior of the generator is given by the matrix equation

$$\mathbf{V} = -\mathbf{R}\mathbf{i} + \mathbf{L}_a \mathbf{i}\frac{da}{dt} - \mathbf{L}_z \frac{d}{dt}\mathbf{i} \tag{4}$$

where $\mathbf{V}$ is the vector of the phase and excitation voltages, $\mathbf{i}$ is the vector of the phase and excitation currents and $\mathbf{R}$ the matrix of the winding resistances: the matrices $\mathbf{L}_a$ and $\mathbf{L}_z$ define the motional and self-inductances of the machine, respectively: the scalar variable a is the angular displacement of the generator shaft $\left(\omega_p \triangleq \frac{da}{dt}\right)$.

An appropriate transformation matrix B transforms the three-phase voltages and currents to two-phase quantities along the direct and quadrature axis of the machine. If a symmetrical three-phase load R_L is connected across the generator terminals, the dynamic behavior of the machine is described by the matrix equation

$$\frac{d}{dt} i_B = -L_z^{-1} R i_B + L_z \omega_p i_B - L_z^{-1} \begin{bmatrix} R_L i_d \\ R_L i_q \\ v_f \end{bmatrix} \tag{5}$$

where the vector i_B is defined by

$$i_B = \begin{bmatrix} i_d \\ i_q \\ i_f \end{bmatrix} \tag{6}$$

with i_d and i_q the direct and quadrature axis currents, respectively. Because of symmetry properties, it is assumed that the zero sequence voltage and current are zero. The equation coupling the electrical to the mechanical machine quantities takes the form

$$\frac{d\omega_p}{dt} = \frac{1}{J_g}\left[T_{IN} - (L_d - L_q)\, i_d i_q - L_5 i_q i_f\right] \tag{7}$$

where J_g is the inertia of the propeller-generator system and L_d, L_q, L_5 are elements of the machine inductance matrices.

Equations (5) and (7) describe the dynamic behavior of the synchronous generator when it is terminated at a symmetrical load R_L and an input torque T_{IN} is applied to its shaft. The model output variables are the direct and quadrature axis currents and the angular velocity of the shaft. Equations (5) and (7) are in state-variable form and

may be solved for the four state variables i_d, i_q, i_f and ω_p using a Runge-Kutta routine.

The steady-state behavior of the machine is arrived at by setting the left-hand side of equations (5) and (7) equal to zero. With the field excitation current, i_f, having reached its final value, v_f/r_f, the functional form of the steady-state equation is

$$\begin{aligned} f_1(i_d, \quad i_q, \omega_p) &= 0 \\ f_2(i_d, \quad i_q, \omega_p) &= 0 \\ f_3(T_{IN}, i_d, \quad i_q) &= 0 \end{aligned} \tag{8}$$

(c) The rectifier circuit A classical bridge rectifier is used to convert the variable frequency ac output of the generator to dc form. Figure 7 shows a simplified schematic of the rectifier circuit. The rectifier is assumed to be loaded by the input impedance of the synchronous inverter, R_{IN}. Thus, the direct and quadrature axis input currents, i_d and i_q, produce an average component of voltage, E, at the rectifier output given by the relation

$$E = 0.7388 R_{IN} \sqrt{i_d^2 + i_q^2} \tag{9}$$

Also, the rectifier load R_{IN}, when reflected to the input side, is linearly related to the generator equivalent load, R_L, by

$$R_L = \frac{R_{IN}}{1.832} \tag{10}$$

Equations (9) and (10) simulate the behavior of the bridge rectifier circuit.

(d) The synchronous inverter A simplified schematic of the inverter circuit is shown in Figure 8. The inverter design and operating characteristics are described in detail elsewhere [13]. It is based upon a four thyristor bridge designed so that an external voltage signal may be used to vary the thyristor firing angle and, therefore, the amount of electrical power being transferred from the wind generator to the utility grid. Variation of the firing angle accomplishes the dynamic matching required for maximum power transfer between the input characteristics of the inverter (dc voltage) and its output characteristics (power grid). The control signal is proportional to the instantaneous power supplied from the WECS to the grid and a feed-back arrangement, as shown in Figure 6, is used to generate a sequence of command voltages which regulate the firing of the thyristors.

A capacitor of large capacitance is connected at the input of the inverter for buffering and smoothing purposes, thus improving the characteristics of the interconnected operation. The inverter is connected to the grid via a filter arrangement which is designed to limit harmonic distortion introduced into the utility system by the pulse shaped inverter output current waveform.

For any given grid impedance, $Z\angle\psi$, at the point of interconnection, the mathematical model for the capacitor-inverter-filter system relates the inverter average power output, P_{out}, to the dc input voltage level, E, and the control signal V_c. The exact mathematical relation is rather lengthy and cumbersome but may be represented, functionally, by

$$P_{out} = g_1(E, V_c, Z\angle\psi) \tag{11}$$

Similarly, the inverter input impedance, R_{IN}, is computed from the same input quantities. This last relation is expressed, in functional form, by

$$R_{IN} = g_2(E, V_c, Z\angle\psi) \tag{12}$$

Equations (11) and (12) define the line-commutated synchronous inverter model.

(e) The power grid The power grid is viewed, at the point of interconnection, as a voltage source of fixed amplitude in series with an impedance $Z\angle\psi$. Values for the grid impedance, at specific grid points where the WECS is to be connected, are calculated from a suitable load flow program.

(f) The protective devices Protective devices are employed for the safe operation of the WECS-grid interconnected system. The wind turbine-generator subsystem is

protected from high wind speeds and excessive generator loadings. The inverter, on the other hand, is operating safely via appropriate devices protecting both the inverter and the grid from various fault conditions. The nature of the overall system design prevents any bi-directional electrical power flow thus eliminating the possible negative consequences of such an operation.

The mathematical models of the safety equipment employed are simple magnitude constraints on certain variables and they are easily implementable during the simulation runs.

(g) Maximum power tracking circuit The feedback circuit includes the following subsystems (Figure 6):

1. An electronic wattmeter that continuously measures the power level at the utility grid terminals and provides a signal output proportional to actual power.
2. A hybrid (analog-digital) power level gradient detector which samples the wattmeter signal output and holds it for comparison with the next sample. The detector includes a comparator that works in combination with a logic circuit to determine whether a given sample represents a power level that is greater or smaller than the previous sample. The logic circuit changes state whenever a new sample is smaller than the preceeding one, but remains in the same state if a new sample is larger than the preceeding one, thus representing an increase in power level.
3. An integrator circuit provides a constantly changing output whose direction of change is increasing for one state of the logic circuit and decreasing for the other state. This control signal is used to fire the inverter thyristors, thus controlling the power level transferred to the grid.

The mathematical model describing the operation of the maximum power tracking device is simply represented by the switching state equations:

$$V_{c_t} = V_{c_{t-1}} \quad \text{if} \quad P_{out_t} > P_{out_{t-1}} \qquad (13)$$
$$V_{c_t} = -V_{c_{t-1}} \quad \text{if} \quad P_{out_t} < P_{out_{t-1}}$$

where $V_c = \pm \upsilon t$ is the control voltage of the line-commutated synchronous inverter (with υ a constant).

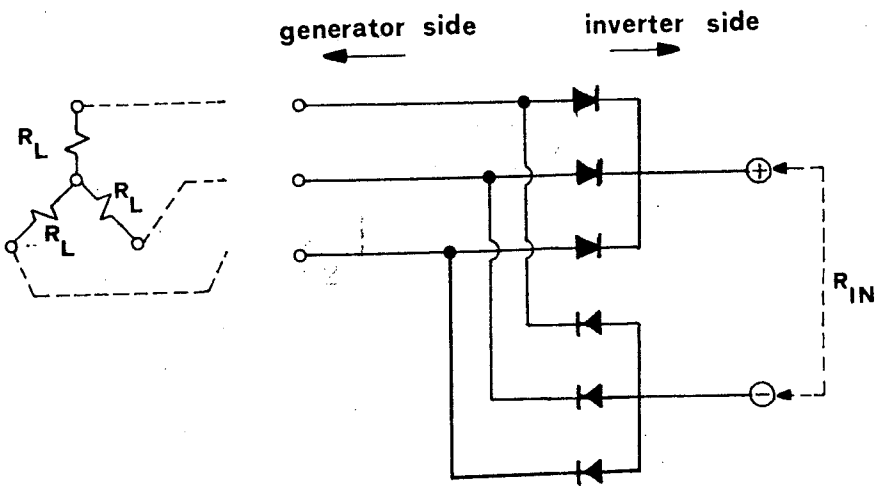

Figure 7 The rectifier circuit

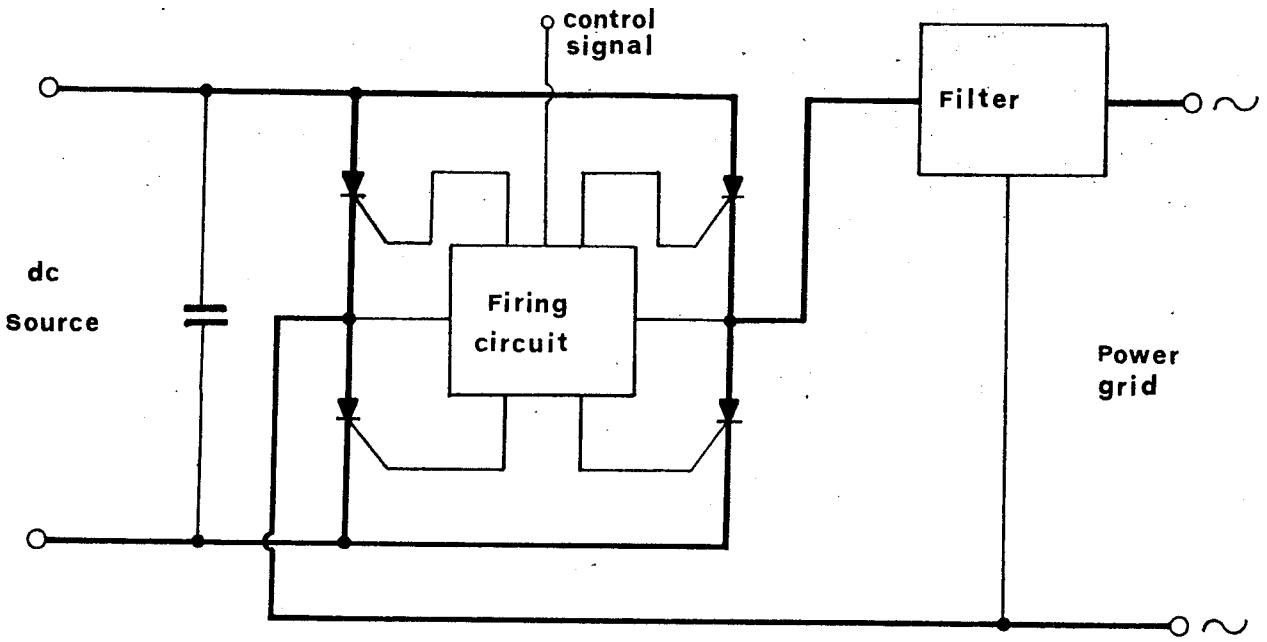

Figure 8 Simplified schematic of the synchronous inverter circuit

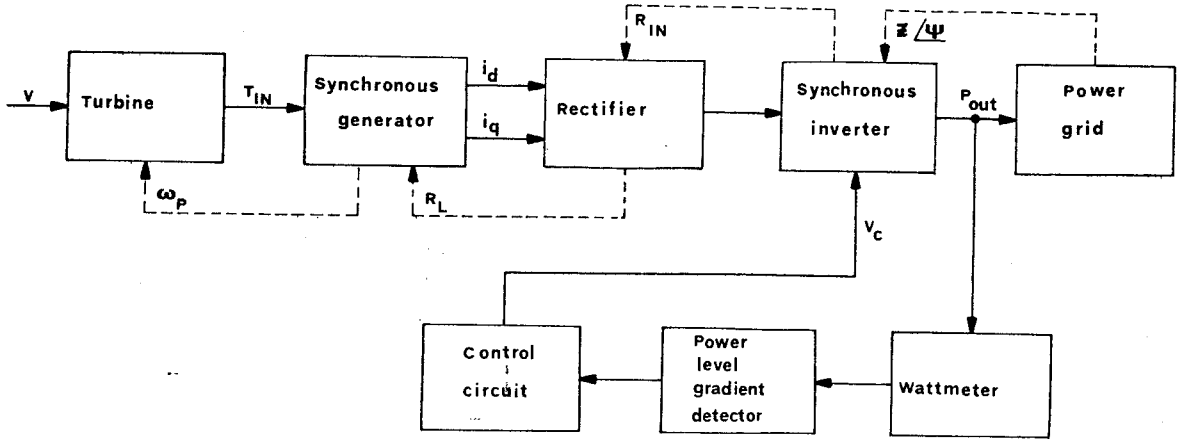

Figure 9 Operational diagram of the interconnected system showing simulation variables

3. The Simulation Study

Figure 9 shows a block diagram of the interconnected system with special attention being given to power flow, control signal and intermediate variable paths. The dynamic synchronous generator model is used first for the study of the transient behavior of the system. Steady-state simulation runs lead to conclusions regarding the effectiveness of the feedback mechanism in maximizing the electrical power transferred to the utility grid.

The simulation proceeds along the following steps:

1. A given thrust change in the wind speed, V, is taken as the input to the model while the grid impedance, $Z\angle\psi$, is assumed to remain constant.
2. The computer program assumes an initial value for the angular speed, ω_p, the input impedance to the inverter, R_{IN} (from which the load R_L, to the generator is calculated) and the control voltage, V_c.
3. The aeroturbine model calculates the shaft output torque, T_{IN}.
4. Next, taking as input quantities the torque, T_{IN}, and the load impedance, R_L, the synchronous generator model calculates the currents i_d and i_q as well as a new value for the angular speed, ω_p.
5. Steps 3 and 4 are repeated with the new values for ω_p until the turbine-generator model reaches a stable condition.
6. Using as input data the last values for i_d and i_q and the initial value for R_{IN}, the voltage input E to the inverter circuit is calculated.
7. In this step, the synchronous inverter model uses as input quantities the voltage level E and the grid impedance $Z\angle\psi$ and computes the power output, P_{out}, and the equivalent impedance R_{IN}. The control voltage level, V_c, is kept temporarily constant.
8. From the computed value for R_{IN}, a new value for R_L is calculated and steps 3 and 4 are repeated until a new stable condition is reached (step 5).
9. Next, steps 6 to 8 are repeated until the turbine-generator-rectifier-inverter model stabilizes.
10. The control voltage level V_c is given a new value and the computational procedure described in steps 3 to 9 is repeated. The two consecutive values for the power output, P_{out}, are used as inputs to the maximum power tracker model whose goal is to set a new value for the control voltage V_c which increases the power output.
11. The computations of steps 3 to 10 are repeated until the power output, P_{out}, oscillates about a maximum value at which instant the program is terminated.

The simulation could be performed without the feedback loop. It is simply terminated at some stable condition of step 9. The firing of the thyristors is accomplished automatically through the connection to the power lines.

Both transient and steady-state runs may be obtained by using the appropriate generator model.

4. Simulation Results

(a) The dynamic behavior For the study of the systems transient behavior, the dynamic model is run with input wind gusts on one hand and sudden changes of the thyristor firing angle on the other. Two types of synchronous generator models are employed: the first one corresponds to a generator whose output impedance is matched to a power line with an impedance of 0.6 Ω and power factor of 0.8 at the point of connection and at approximately the rated speed of the machine, while the second represents a generator whose characteristics match a line of 5 mΩ impedance at 0.57 power factor.

Figure 10 shows the computer simulation results when the first type of generator is used. The input signal is originally a step change in wind speed from 0 to 10 m/sec. The excitation remains at the 10 m/sec level until the system behavior reaches steady-state conditions (approximately 120 sec). At that moment, the wind speed is reduced from 10 m/sec to 5 m/sec and the simulation is repeated using the previous steady-state values as the new model initial conditions. The results indicate that transient phenomena proceed smoothly without a need to initiate the operation of any protective devices. Similar runs with various wind speed input functions lead to parallel conclusions as far as the transient behavior is concerned.

It is noted that the time constant of the mechanical subsystem is of the order of several seconds. Thus, the time constants associated with the electrical subsystem

(response times of the order of msec) may be neglected when compared with the mechanical subsystem response. As a conclusion it may be stated that the system is electrically in a steady-state condition at each instant of time. The steady-state model of the synchronous generator may, therefore, be used in the study of power transfer phenomena.

Figure 11 depicts the transient behavior of several system variables when the thyristor firing angle is subjected to a series of sudden changes – 100 μsec, 200 μsec and 300 μsec. The wind speed remains constant at 10 m/sec. It is evident again from Figure 11 that changes in the firing angle do not cause any transient stability problems.

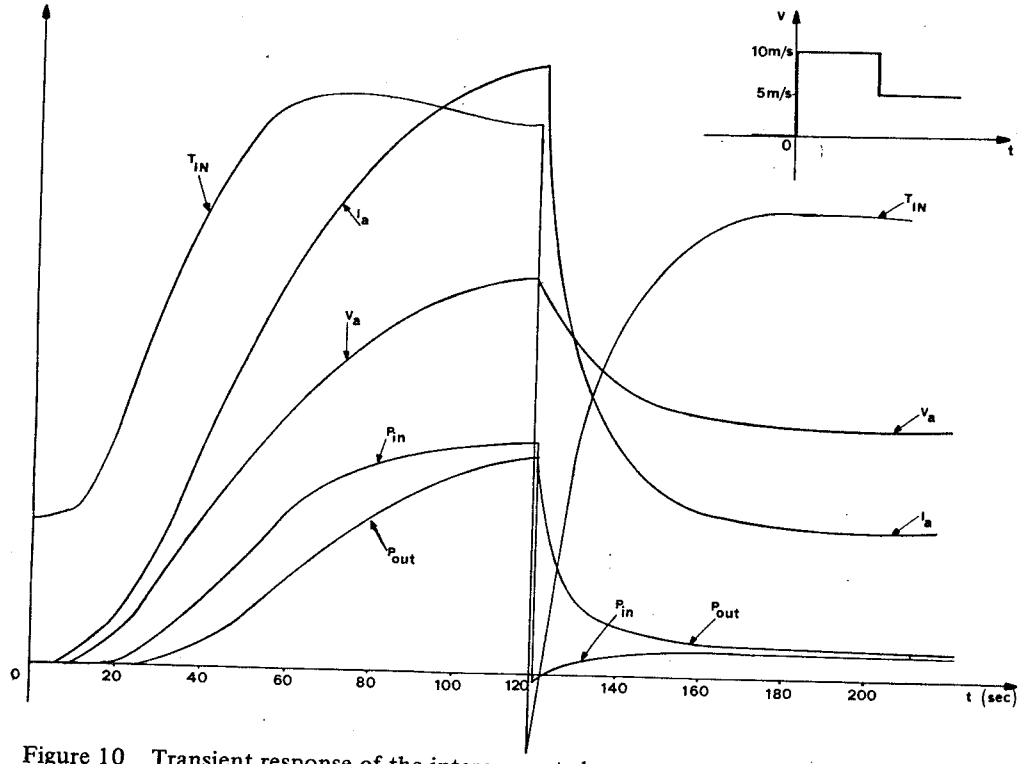

Figure 10 Transient response of the interconnected system variables. The wind input excitation is shown at the top right

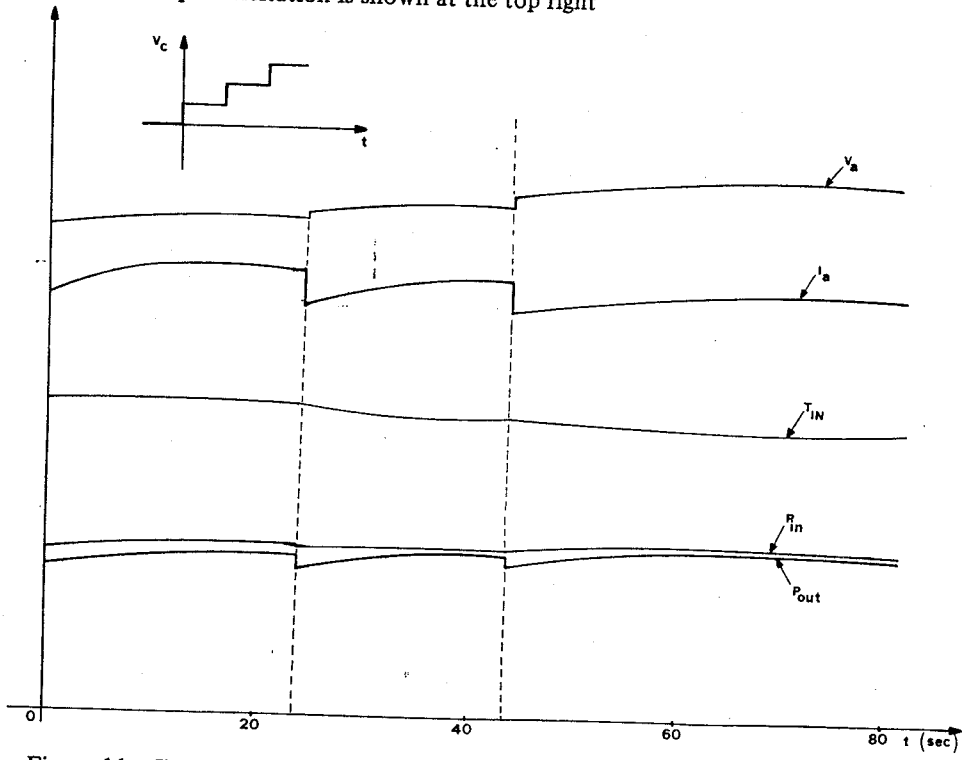

Figure 11 Transient system behavior with constant wind speed and a step change in the firing voltage

(b) The steady-state behavior This study involves two particular cases: firstly, the wind speed is varied while the grid impedance is kept constant and secondly, the wind speed is kept constant while the grid impedance is varied. Both the unmatched and matched generator models are employed in the simulation runs when the WECS is connected to a power grid with specified characteristics. The system model is considered first with the feedback loop open and subsequently with the loop closed. Thus, the combinations of simulation runs produce the four power output curves of Figure 12. It is observed that the power transfer efficiency improves by as much as 80% for the unmatched model whereas the improvement is about 5% for the matched case with the maximum power tracking mechanism in operation.

It is also noteworthy that the curves corresponding to maximum power being transferred from the two types of machine models coincide. This implies that the maximum power transfer scheme achieves always the maximum power transfer for the interconnected system.

A second category of simulation runs involves keeping the wind speed constant at 10 m/sec and varying the grid impedance from 4 to 40 mΩ with $\cos\varphi = 0.57$. This region covers all usual load variations of a small autonomous power system. The computer results are shown in Figure 13. The power transfer efficiency shows an improvement ranging from 68 to 55% over the range of interest for the unmatched case whereas the improvement is rather insignificant for the matched system.

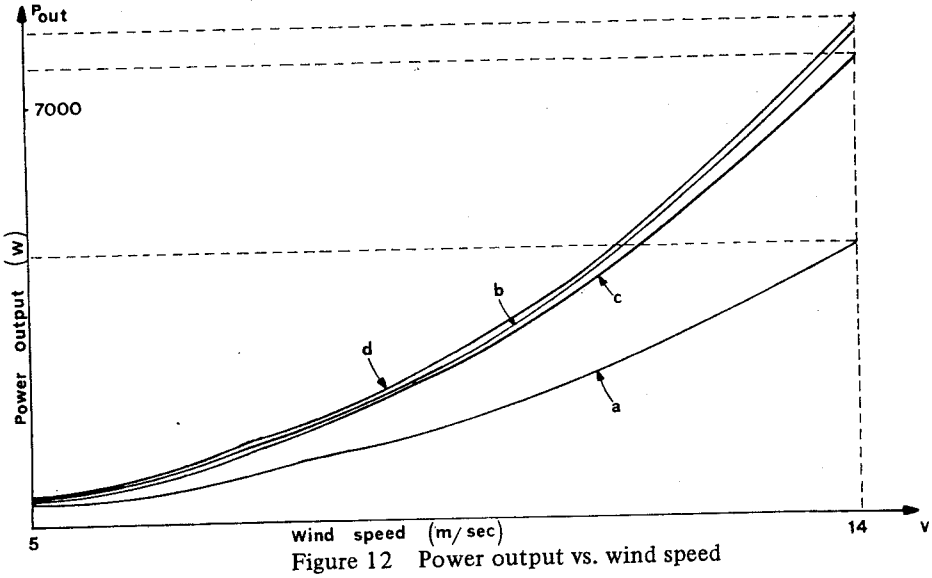

Figure 12 Power output vs. wind speed

(a) – unmatched system without feedback
(b) – " " with "
(c) – matched " without "
(d) – " " with "

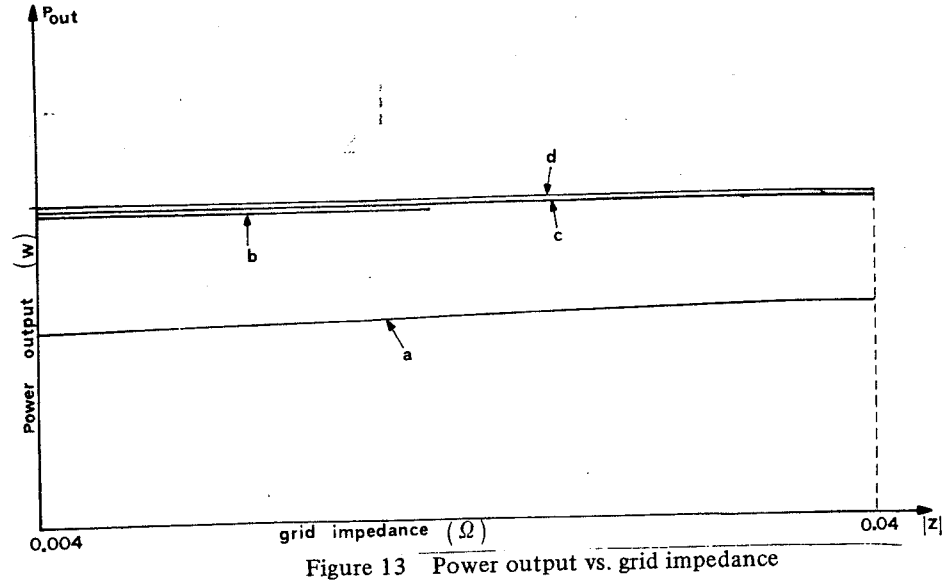

Figure 13 Power output vs. grid impedance

(a) – unmatched system without feedback
(b) – " " with "
(c) – matched " without "
(d) – " " with "

5. Conclusions

The dynamic behavior of the interconnected system reveals no undesirable transient phenomena such as mechanical oscillations or over-voltages and currents. These results are also verified by experimentation. Thus, the requirements for mechanical and electrical endurance of the particular WECS studied are not severe, with obvious consequences for system costs.

The safety equipment protects effectively both the wind generator and the power grid from various fault conditions.

Both impedance matching and power tracking result in maximization of the energy transferred from the WECS to the grid.

These results, coupled with the fact that a simple and inexpensive synchronous generator is employed, indicate that an optimum operation, from a technical and economic standpoint, is achieved for a large range of wind speed variations.

Finally, the low cost of components (inverter-tracker) and maintenance adds to the economic attractiveness of the proposed scheme.

References

1. **T.S. Jayadev.** *"Windmills Stage a Comeback", IEEE Spectrum, November 1976.*

2. **Lenard Larsson.** *"Large Scale Introduction of Wind Power Stations in the Swedish Grid: A simulation study", Wind Engineering, Vol.2, No.4, 1978.*

3. **T.W. Reddoch, J.W. Klein.** *"No Ill Winds for New Mexico Utility", IEEE Spectrum, pp 57-61, March 1979.*

4. **Harry Davitian.** *"Wind Power and Electric Utilities: A Review of the Problems and Prospects", Wind Engineering, Vol.2, No.4, 1978.*

5. **Edward Kahn.** *"The Reliability of Distributed Wind Generators", Electric Power Systems Research, pp 1-14, Vol.2, 1979.*

6. **C.J. Todd, P.L. Eddy, R.C. James, W.E. Howell.** *"Cost Effective Electric Power Generation from the Wind: A System Linking Wind Power with Hydroelectric Storage and Long Distance Transmission", Wind Engineering, Vol.2, No.1, 1978.*

7. **Leslie Braunstein.** *"Wind Energy: The Long Road to Commercialization", Energy, Winter 1979.*

8. **R.A. Schlueter, G.L. Park, H. Modir, J. Dorsey, M. Lotfalian.** *"Assessment of the Effects of Large Wind Generator Arrays on Power System Operation", IEEE PES Winter Meeting, New York, N.Y., Feb. 3-8, 1980.*

9. **G.H. Bontius, A.H.E. Manders, Th. Stoop.** *"Implications of Large Scale Introduction of Power from Large Wind Energy Conversion Systems into the Existing Electric Power Supply System in the Netherlands", 2nd International Symposium on Wind Energy Systems, October 3rd--6th, 1978.*

10. **B.T. Ooi and R.A. David.** *"Induction-Generator/Synchronous-Condenser System for Wind Turbine Power", Proceedings of IEEE, Vol.126, No.1, January 1979.*

11. **R. Ramakumar.** *"Wind-Electric Conversion Utilizing Field Modulated Generator Systems", Solar Energy, Vol.20, pp 109-177, Pergamon Press, 1978.*

12. **R. Ramakumar.** *"Idealized Model of Field Modulated Generator Systems: an Experimental Study", Midwest Power Symposium, Manhattan, Kansas, October 7-8, 1976.*

13. **G.J. Vachtsevanos, K.C. Kalaitzakis.** *"A Synchronous Inverter for Wind Energy Conversion Systems", Melecon 81, Tel Aviv, Israel, 1981.*